Alexandria Engineering Journal (2016) 55, 203–214

Alexandria University

Alexandria Engineering Journal

www.elsevier.com/locate/aej
www.sciencedirect.com

ORIGINAL ARTICLE

Modeling of MHD natural convection in a square enclosure having an adiabatic square shaped body using Lattice Boltzmann Method

Ahmed Kadhim Hussein [a,*], **H.R. Ashorynejad** [b], **S. Sivasankaran** [c], **Lioua Kolsi** [d,e], **M. Shikholeslami** [b], **I.K. Adegun** [f]

[a] *Department of Mechanical Engineering, College of Engineering, Babylon University, Babylon City, Iraq*
[b] *Faculty of Mechanical Engineering, Babol University of Technology, Babol, Islamic Republic of Iran*
[c] *Institute of Mathematical Sciences, University of Malaya, Kuala Lumpur 50603, Malaysia*
[d] *Unité de recherche de Métrologie et des Systèmes Energétiques, Ecole Nationale d'Ingénieurs, Université de Monastir, 5000 Monastir, Tunisia*
[e] *College of Engineering, Mechanical Engineering Department, Haïl University, Haïl City, Saudi Arabia*
[f] *Department of Mechanical Engineering, University of Ilorin, Ilorin, Nigeria*

Received 30 March 2015; revised 3 December 2015; accepted 5 December 2015
Available online 7 January 2016

KEYWORDS

Natural convection;
Magneto-hydrodynamics;
Adiabatic body;
Lattice Boltzmann Method

Abstract A steady laminar two-dimensional magneto-hydrodynamics (MHD) natural convection flow in a square enclosure filled with an electrically conducting fluid is numerically investigated using Lattice Boltzmann Method (LBM). The left and right vertical sidewalls of the square enclosure are maintained at hot and cold temperatures respectively. The horizontal top and bottom walls are considered thermally insulated. An adiabatic square shaped body is located in the center of a square enclosure and an external magnetic field is applied parallel to the horizontal *x*-axis. In the present work, the following parametric ranges of the non-dimensional groups are utilized: Hartmann number is varied as $0 \leqslant Ha \leqslant 50$, Rayleigh number is varied as $10^3 \leqslant Ra \leqslant 10^5$, Prandtl number is varied $0.05 \leqslant Pr \leqslant 5$. It is found that the Hartmann number, Rayleigh number, and Prandtl number have an important role on the flow and thermal characteristics. It is found that when the Hartmann number increases the average Nusselt number decreases. The results also explain that the effect of magnetic field on flow field increases by increasing Prandtl number. However, the Prandtl number effect on the average Nusselt number with a magnetic field is less than the case without a magnetic field. Comparisons with previously published numerical works are performed and good agreements between the results are observed.

© 2015 Faculty of Engineering, Alexandria University. Production and hosting by Elsevier B.V. This is an open access article under the CC BY-NC-ND license (http://creativecommons.org/licenses/by-nc-nd/4.0/).

* Corresponding author.
E-mail address: ahmedkadhim7474@gmail.com (A.K. Hussein).

Peer review under responsibility of Faculty of Engineering, Alexandria University.

http://dx.doi.org/10.1016/j.aej.2015.12.005
1110-0168 © 2015 Faculty of Engineering, Alexandria University. Production and hosting by Elsevier B.V.
This is an open access article under the CC BY-NC-ND license (http://creativecommons.org/licenses/by-nc-nd/4.0/).

Nomenclature

B	strength of the magnetic field (tesla)
c_i	discrete lattice velocity in i-direction
c_s	speed of sound (m/s)
F_k	external force in lattice velocity direction
f_i^{eq}	density equilibrium function
g_y	gravitational acceleration (m/s^2)
g	distribution function
Gr	Grashof number (Ra × Pr)
H	height of the enclosure (m)
Ha	Hartmann number
h_i^{eq}	magnetic equilibrium function
L	length of the square enclosure (m)
Nu	Nusselt number
Pr	Prandtl number
p	pressure (N/m^2)
Ra	Rayleigh number
u	horizontal velocity component (m/s)
$V_{natural}$	characteristic velocity of the flow for natural regime (m/s)
v	vertical velocity component (m/s)
w	length of adiabatic square body (m)
w_i	weighting factor
x	cartesian coordinate in horizontal direction (m)
y	cartesian coordinate in vertical direction (m)

Greek symbols

α	thermal diffusivity (m^2/s)
β	volumetric thermal expansion coefficient (K^{-1})
η	magnetic resistivity (m^2/s)
θ	temperature distribution
λ_i	weighting factor of magnetic field
σ	electrical conductivity (W/m °C)
μ	dynamic viscosity (kg/m s)
υ	kinetic viscosity (m^2/s)
ψ	stream function
ρ	density (kg/m^3)
Δt	lattice time step
ΔT	temperature difference (°C)
γ	magnetic field direction
τ_v	lattice relaxation time for the flow field
τ_c	lattice relaxation time for the temperature field
τ_m	lattice relaxation time for the magnetic field

Subscripts

ave	average
Max	maximum

Abbreviations

BGK	Bhatnagar–Gross–Krook approximation
D2Q9	two-dimensional nine-velocity model
MHD	magneto-hydrodynamics
LBE	Lattice Boltzmann Equation
LBM	Lattice Boltzmann Method

1. Introduction

The term magneto-hydrodynamics (MHD) or sometimes called 'magneto-convection' summarizes the variety of processes arising from the dynamic interaction between convective motions and magnetic fields in an electrically conducting medium. MHD natural convection flows are encountered in numerous problems with technological and industrial interest, covering a wide range of basic sciences such as astrophysics, fire research, metallurgy, crystal growth and nuclear engineering [1]. Natural convection flows are characterized by a balance between a pressure drop and buoyancy forces. In MHD natural convection flows, the balance is achieved by inertial, viscous, electromagnetic and buoyancy forces, making the solution more complicated. Analytic and asymptotic solutions are known only for simple geometries under the restriction of two-dimensional viewing. Recently, MHD natural convection flows have much attention because the process of manufacturing materials in industrial problems and microelectronic heat transfer devices involves an electrically conducting fluid subjected to magnetic field. In this case the fluid experiences a Lorentz force and its effect is to reduce the flow velocities which affects the heat transfer rate [2,3]. Many numerical and experimental methods have been developed to investigate the flow characteristics inside enclosures with and without a fixed body at their centers. These geometries have realistic engineering and industrial purposes, for example in the design of solar collectors, thermal design of building, air conditioning, cooling of electronic devices, furnaces, lubrication technologies, chemical processing equipment, drying technologies. Extensive research works have been published on MHD natural convection heat transfer in enclosures with and without a fixed body under different conditions by Garandet et al. [4], Ozoe and Okada [5], Rudraiah et al. [6], Cowley [7], Al-Najem et al. [8], Teamah [9], Ece and Buyuk [10] and Jalil and Al-Tae'y [11]. Furthermore, Saravanan and Kandaswamy [12] investigated convection in a low Prandtl number fluid driven by the combined mechanism of buoyancy and surface tension in the presence of a uniform vertical magnetic field. The fluid was contained in a square cavity with the upper surface open and isothermal vertical walls. The thermal conductivity of the fluid was assumed to vary linearly with temperature. The heat transfer was found to decrease appreciably across the cavity with a decrease in thermal conductivity. The accumulation of streamlines by Lorentz force was seen for linearly varying thermal conductivity. Gelfgat and Bar-Yoseph [13] considered the problem of onset of oscillatory instability in convective flow of an electrically conducting fluid under an externally imposed time-independent uniform magnetic field. Convection of a low-Prandtl number fluid in a laterally heated two-dimensional horizontal cavity was investigated. Fixed values of the aspect ratio (length/height = 4) and Prandtl number (Pr = 0.015) are considered. The effect of a uniform magnetic field with different magnitudes and orientations on the stability of the two distinct branches (with a single-cell or a two-cell pattern) of the steady state flows was also investigated. It was shown that a

vertical magnetic field provided the strongest stabilization effect, and also that multiplicity of steady states was suppressed by the electromagnetic effect, so that at a certain field level only the single-cell flows remain stable. Aleksandrova and Molokov [14] considered three-dimensional convection in a rectangular cavity subjected to a horizontal temperature gradient and a magnetic field, by an asymptotic model. They concluded that the effectiveness of the application of the magnetic field depended considerably on the aspect ratio and the value of the Hartmann number. Hof et al. [15] presented an experimental study of the effect of the magnetic field on the natural convection stability in a rectangular cavity of square section, filled with a liquid metal. They found that the vertical direction of the magnetic field was most effective for the suppression of oscillations. Lee and Ha [16] investigated numerically the natural convection in a horizontal enclosure with an interior conducting body and compared the results of conducting body with those of adiabatic and isothermal bodies. They concluded that when the Rayleigh number was less than 10^4, the effect of the convection on the fluid flow and heat transfer was relatively weak and the Nusselt number on the bottom hot wall was depended on the variation of the thermal conductivity ratio. From the other hand, they found that when the Rayleigh number was larger than 10^5, the effect of the convection became more dominant and the Nusselt number on the bottom hot wall did not depend so much on the variation of the thermal conductivity ratio. Jalil et al. [17] performed a numerical three-dimensional study on the turbulent natural convection of molten sodium (low Prandtl number fluid) in a cubic cavity heated from one vertical wall and cooled from an opposing vertical wall, with the other walls thermally insulated. The cavity was exposed to external uniform magnetic fields, either horizontal or perpendicular, to the heated wall (x-direction) or in vertical and parallel directions to the heated wall (y-direction) or in horizontal and parallel directions to the heated wall (z-direction). The magnetic field in the horizontal and perpendicular directions gave the smallest value of the average Nusselt number on the vertical heated wall and in the vertical and parallel directions the largest value. On the other hand, the external magnetic field in horizontal and parallel directions was found to be effective in between these two extremes. The effect of magnetic field on Nusselt number in the three-dimensional laminar flow was greater than that for two-dimensional laminar flow at the same value of the magnetic field intensity.

Ece and Büyük [18] considered steady, laminar, natural-convection flow in the presence of a magnetic field in an inclined square enclosure differentially heated along the bottom and left vertical walls while the other walls were kept isothermal. The governing equations were solved numerically for various Grashof and Hartmann numbers, inclination angle of the enclosure and direction of the magnetic field. They concluded that magnetic field suppressed the convective flow and its direction also influenced the flow pattern, causing the appearance of inner loops and multiple eddies. Henry et al. [19] studied numerically the directional effect of a magnetic field on the onset of oscillatory convection in a confined three-dimensional cavity filled with mercury and subjected to a horizontal temperature gradient. They concluded that the magnetic field suppressed the oscillations most effectively when it was applied in the vertical direction, and was the least efficient when applied in the longitudinal direction parallel to the temperature gradient. Pirmohammadi and Ghassemi [20] investigated numerically using finite volume code of steady, laminar, natural-convection flow in the presence of a magnetic field in a tilted liquid gallium filled enclosure heated from below and cooled from top. It was shown that for a given inclination angle (φ), as the value of Hartmann number (Ha) increased, the convection heat transfer reduced. Furthermore, it was found that at $Ra = 10^4$, value of Nusselt number depended strongly upon the inclination angle for relatively small values of Hartmann number. At $Ra = 10^5$, the Nusselt number increased up to $\varphi = 45°$ and then decreased as the inclination angle increased. Ashorynejad et al. [21] presented a numerical study of the magnetohydrodynamic flow in a square cavity filled with porous medium by using Lattice Boltzmann Method. The left and right vertical walls of the cavity were kept at constant but different temperatures while both the top and bottom horizontal walls were insulated. The results explained that heat and mass transfer mechanisms and the flow characteristics inside the enclosure depended strongly on the strength of the magnetic field and Darcy number. They concluded that, the average Nusselt number decreased with increasing values of the Hartmann number while it increased with increasing values of the Darcy number. Nasrin [22] performed a computational study by using finite element simulation to investigate the effect of Joule heating on hydromagnetic free convective flow and heat transfer characteristics in a square enclosure with a heated horizontal circular obstacle located at the center. The obstacle was maintained at constant temperature (T_h). The left vertical surface of the cavity was uniformly heated of temperature (T_c) while the other three surfaces were considered thermally insulated. The behavior of the fluid was studied in the ranges of Prandtl number (0.073–2.73), Hartmann number (0–50) and Joule heating parameter (1–7). He concluded that the heat transfer rate increased with rising Prandtl number while it devalues for mounting Hartmann number and Joule heating parameter. Very recently, Sheikhzadeh et al. [23] numerically investigated using the control volume method the effects of Prandtl number on the steady magneto-convection around a centrally located adiabatic body inside a square enclosure. The results were displayed in the form of streamlines and isotherms when the Rayleigh number varied between 10^3 and 10^6, the Hartmann number varied between 0 and 100 and the Prandtl number varied between 0.005 and 0.1. They concluded that the Prandtl number had no considerable effect on heat transfer at low Rayleigh numbers. The effect of magnetic field strength on convection was increased by increasing the Prandtl number while the effect of Prandtl number on the average Nusselt number in the presence of a magnetic field was less than the case without a magnetic field. Another useful researches had been conducted to simulate the MHD natural convection under different conditions can be found in [24–31]. From the other hand, the Lattice Boltzmann Method (LBM) is a new method for simulating fluid flow and modeling physics in fluids [32–34]. This method has also been successfully applied to flow in porous media and MHD flow [21]. In general, to our best knowledge, magneto-hydrodynamics natural convection flow around an adiabatic square body located inside the center of square enclosure using the Lattice Boltzmann Method has not been considered in any paper previously. Thus, the main purpose of this paper is to examine this problem in detail. The effects of Rayleigh number, Hartmann number and

Prandtl number on streamlines, isotherms and the Nusselt number are investigated.

2. Mathematical modeling

2.1. Governing equations and geometrical configuration

The steady magneto-hydrodynamic natural convection flow around an adiabatic square body of dimensions ($w \times w$) located inside the center of square enclosure of dimensions ($L \times L$) filled with an electrically conducting fluid is considered as shown in Fig. 1 along with the important geometric parameters. The body size to the height of the enclosure (w/L) is considered constant as 0.5. The vertical left and right sidewalls of square enclosure are maintained at constant hot and cold temperatures respectively while the horizontal top and bottom walls are considered thermally insulated together with the interior square body. A uniform external magnetic field of strength (B) is applied parallel to the horizontal x-axis. The Hartmann number (Ha) is varied as 0, 10 and 50, the Rayleigh number (Ra) is varied as 10^3, 10^4 and 10^5 to cover both buoyancy and magnetic field dominant flow regimes, and the Prandtl number (Pr) is varied as 0.05, 0.5 and 5 respectively. In the present work, the following assumptions are used:

- Steady laminar two-dimensional flow, i.e. variation in z-direction is neglected.
- Incompressible regime is considered.
- Gravity acts vertically downward.
- Newtonian fluid.
- Viscous dissipation is considered to be neglected.
- The Boussinesq approximation is applied and radiation heat transfer is negligible.

The classic continuity, momentum and energy equations for MHD natural convection are written as follows in terms of the macroscopic variables:

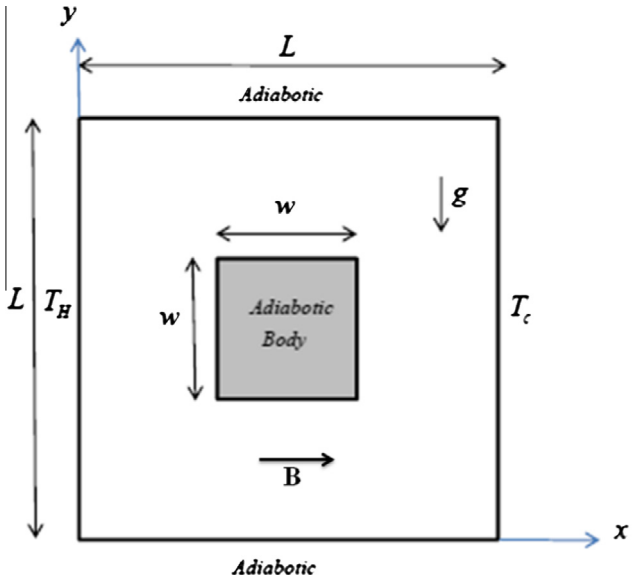

Figure 1 Geometry and coordinates of square enclosure with an adiabatic square shaped body in the presence of magnetic field.

$$\frac{\partial u}{\partial x}+\frac{\partial v}{\partial y}=0 \tag{1}$$

$$\rho\left(u\frac{\partial u}{\partial x}+v\frac{\partial u}{\partial y}\right)=-\frac{\partial p}{\partial x}+\mu\left(\frac{\partial^2 u}{\partial x^2}+\frac{\partial^2 u}{\partial y^2}\right)+F_x \tag{2}$$

$$\rho\left(u\frac{\partial v}{\partial x}+v\frac{\partial v}{\partial y}\right)=-\frac{\partial p}{\partial y}+\mu\left(\frac{\partial^2 v}{\partial x^2}+\frac{\partial^2 v}{\partial y^2}\right)+F_y \tag{3}$$

where F_x, F_y are the total body forces at x and y directions respectively and they are defined as follows:

$$F_x=\frac{\mathrm{Ha}^2\mu}{L^2}(v\sin\gamma\cos\gamma-u\sin^2\gamma) \tag{3-a}$$

and

$$F_y=\rho g\beta(T-T_c)+\frac{\mathrm{Ha}^2\mu}{L^2}(u\sin\gamma\cos\gamma-v\cos^2\gamma) \tag{3-b}$$

where γ is the magnetic field direction

$$u\frac{\partial T}{\partial x}+v\frac{\partial T}{\partial y}=\alpha\left(\frac{\partial^2 T}{\partial x^2}+\frac{\partial^2 T}{\partial y^2}\right) \tag{4}$$

2.2. Lattice Boltzmann Equations for flow, thermal and magnetic fields

The Lattice Boltzmann Method (LBM) is a microscopic method originates from the lattice-gas automata method, and can also be viewed as a special discrete scheme for the Boltzmann equation with discrete velocities. In LBM, the fluid is modeled as a collection of particles moving on a uniform, square grid. Particles are placed on the nodes of the grid and move from some nodes where they are located toward the neighboring node between two instants. The Lattice Boltzmann model used in the present work is the same as that employed in Cramer and Pai [35]. The thermal Lattice Boltzmann model utilizes two distribution functions, f, g and B, for the flow, temperature and magnetic fields, respectively. It uses modeling of movement of fluid particles to capture macroscopic fluid quantities such as velocity, pressure, temperature and magnetic field. In this approach, the fluid domain was discretized to uniform Cartesian cells. Each cell holds a fixed number of distribution functions, which represent the number of fluid particles moving in these discrete directions. The density and distribution functions (i.e., the f, g and B) are calculated by solving the Lattice Boltzmann Equation (LBE), which is considered as a special discretization of the kinetic Boltzmann equation. After introducing B hatnagar–Gross–Krook (BGK) approximation, the general form of Lattice Boltzmann Equation with external force is as follows:

For the flow field:

$$f_i(x+c_i\Delta t,t+\Delta t)=f_i(x,t)+\frac{\Delta t}{\tau_v}\left[f_i^{eq}(x,t)-f_i(x,t)\right]+\Delta t c_i F_k \tag{5}$$

For the temperature field:

$$g_i(x+c_i\Delta t,t+\Delta t)=g_i(x,t)+\frac{\Delta t}{\tau_C}[g_i^{eq}(x,t)-g_i(x,t)] \tag{6}$$

where Δt denotes lattice time step, c_i is the discrete lattice velocity in direction i, F_k is the external force in direction of lattice velocity, τ_v and τ_c denote the lattice relaxation time for the flow and temperature fields respectively. In order to incorporate buoyancy forces and magnetic forces in the model, the force term (F_k) in the Eq. (5) needs to be calculated as below:

$$F_k = F_x + F_y \tag{7}$$

The kinematic viscosity (υ) and the thermal diffusivity (α), are defined in terms of their respective relaxation times, i.e., ($\upsilon = c_s^2(\tau_v - 1/2)$) and ($\alpha = c_s^2(\tau_C - 1/2)$) respectively. Note that the limitation $0.5 < \tau$ should be satisfied for both relaxation times to ensure that the viscosity and the thermal diffusivity are positive. In fact, the local equilibrium distribution function has an appropriately prescribed functional dependence on the local hydrodynamic properties. It also models the equilibrium distribution functions for the flow and temperature fields respectively.

In this study, the density distribution function, f_i^{eq}, was modified to consider the magnetic effect:

$$f_i^{eq} = w_i\rho\left[1 + \frac{c_i \cdot u}{c_s^2} + \frac{1}{2}\frac{(c_i \cdot u)^2}{c_s^4} - \frac{1}{2}\frac{u^2}{c_s^2}\right] + \frac{w_i}{2c_s^2}\left[\frac{B^2c^2}{2} - (c \cdot B)^2\right] \tag{8}$$

$$g_i^{eq} = w_i T\left[1 + \frac{c_i \cdot u}{c_s^2}\right] \tag{9}$$

where B is the magnetic field, w_i is weighting factor, c_s is the speed of sound and defined by $c_s = \frac{c}{\sqrt{3}}$. The density Lattice Boltzmann thermal model or two-dimensional nine-velocity model (D2Q9) was used and values of $w_0 = 4/9$ for $|c_0| = 0$ (for the static particle), $w_{1-4} = 1/9$ for $|c_{1-4}| = 1$ and $w_{5-9} = 1/36$ for $|c_{5-9}| = \sqrt{2}$ are assigned in this model. Similarly, to density equilibrium function $\left(f_i^{eq}\right)$, for calculating the magnetic field, magnetic equilibrium function (h_i^{eq}) is considered as following (Dellar [36]):

$$h_{ix}^{eq} = \lambda_i\left[B_x + \frac{1}{c_s^2}e_{ix}(u_yB_x - u_xB_y)\right] \tag{10}$$

$$h_{iy}^{eq} = \lambda_i\left[B_y + \frac{1}{c_s^2}e_{iy}(u_xB_y - u_yB_x)\right] \tag{11}$$

where (λ_i) is the weighting factor of magnetic field and defined in fifth direction by (Dellar [36]):

$$\lambda_i = \begin{cases} \frac{1}{3} & \text{for } i = 0 \\ \frac{1}{6} & \text{for } i = 1-4 \end{cases} \tag{12}$$

For solving the velocity and magnetic field, the following equation must be considered (Dellar [36]):

$$h_i(x + c_i\Delta t, t + \Delta t) = h_i(x,t) + \frac{\Delta t}{\tau_m}\left[h_i^{eq}(x,t) - h_i(x,t)\right] \tag{13}$$

The magnetic resistivity (η), like kinematic viscosity (υ) and the thermal diffusivity (α), which is defined in terms of its respective relaxation time (τ_m) $\left[\left(\eta = c_s^2(\tau_m - 1/2)\Delta t\right)\right]$. Where ($\tau_m$) is the lattice relaxation time for the magnetic field.

In order to incorporate buoyancy force in the model, the force term in the Eq. (1) needs to be calculated in the vertical direction (y) as follows:

$$F = 3w_ig_y\beta\theta \tag{14}$$

For natural convection, the Boussinesq approximation is applied and radiation heat transfer is negligible. To ensure that the code works near incompressible regime, the characteristic velocity of the flow for natural regime ($V_{natural} \equiv \sqrt{\beta g_y \Delta T H}$) must be small compared with the fluid speed of sound. In the present study, the characteristic velocity selected as 0.1 of sound speed. Finally, the macroscopic variables were calculated using the following formula:

$$\rho = \sum_i f_i, \quad \rho u = \sum_i c_i f_i, \quad T = \sum_i g_i,$$
$$B_x = \sum_i h_{ix}, \quad B_y = \sum_i h_{iy} \tag{15}$$

The Hartmann number, Rayleigh number, Prandtl number and the Grashof number can be defined respectively as follows:

$$\mathrm{Ha} = B \times H\sqrt{\sigma/\mu}, \quad \mathrm{Ra} = \frac{g_y\beta\Delta T H^3}{\nu \cdot \alpha},$$
$$\mathrm{Pr} = \frac{\nu}{\alpha} \quad \text{and} \quad \mathrm{Gr} = \mathrm{Ra} \times \mathrm{Pr} \tag{16}$$

The average Nusselt number (Nu_{ave}) is one of the most important dimensionless parameters in describing the convective heat transport. It is computed at the hot wall (left sidewall) as follows:

$$\mathrm{Nu}_{ave} = \int_0^1 \frac{\partial\theta}{\partial x}dy \quad (\text{at } x = 0) \tag{17}$$

Finally, the lattice relaxation times for the temperature, flow and magnetic fields are defined respectively as follows:

$$\tau_c = \frac{\alpha}{c_s^2\Delta t} + \frac{1}{2} \tag{18}$$

$$\tau_v = \frac{\nu}{c_s^2\Delta t} + \frac{1}{2} \tag{19}$$

$$\tau_m = \frac{\eta}{c_s^2\Delta t} + \frac{1}{2} \tag{20}$$

2.3. Boundary conditions

The implementation of boundary conditions is very important for the simulation. The distribution functions out of the domain are known from the streaming process. The unknown distribution functions are those toward the domain. Bounce-back boundary conditions were applied on all solid boundaries, which mean that incoming boundary populations equal to outgoing populations after the collision. The boundary conditions of the top and bottom walls are all adiabatic. The initialization conditions of the four walls of the enclosure are given as follows:

- No-slip boundary condition are applied at all enclosure boundaries (i.e., $u = v = 0$)
- The left vertical sidewall is subjected to an isothermal hot temperature (T_h), i.e.,

at $x = 0, \quad T = T_h$

- The right vertical sidewall is subjected to an isothermal cold temperature (T_c), i.e.,

at $x = 1, \quad T = T_c$

The top and the bottom walls are considered adiabatic, i.e.,

$$\text{at } y = 0 \text{ and } y = 1, \quad \frac{\partial T}{\partial y} = 0 \tag{21}$$

From the other hand, the boundary conditions of the internal square body is given by the following:

at $x = w, \quad \frac{\partial T}{\partial x} = 0$

and at $y = w, \quad \frac{\partial T}{\partial y} = 0$

No-slip boundary condition are applied at all internal square body boundaries ($u = v = 0$).

3. Results and discussion

Table 1 illustrates the effect of grid sizes (20 × 20), (40 × 40), (60 × 60), (80 × 80) and (100 × 100) for Ra = 10^3, Ra = 10^4 and Ha = 0 by calculating the average Nusselt number at the hot left sidewall. It was found that a grid size of (80 × 80) ensures a grid independent solution. To check the validity of the numerical simulation, a comparison is performed between the results obtained by the present computer code with the results of Rudraiah et al. [6], for Gr = 2 × 10^4 and Gr = 2 × 10^5. Fig. 2 shows the effect of a transverse magnetic field on natural-convection flow inside a rectangular enclosure which is compared with the result of Rudraiah et al. [6]. The comparison shows an excellent agreement between the results obtained by present computer code with the results of Rudraiah et al. [6]. After that, the magneto-hydrodynamic natural convection phenomenon with Prandtl number effect inside a square enclosure having an adiabatic square body is numerically studied. The influence of various controlling parameters such as Hartmann number, Rayleigh number and Prandtl number on the flow and thermal fields was performed. Flow and heat transfer characteristics, streamlines, isotherms and average Nusselt number are presented and discussed in this section. Analysis of the results is made through obtained streamlines, isotherms and average Nusselt number for three dimensionless parameters varied as $0.05 \leqslant Pr \leqslant 5$, $0 \leqslant Ha \leqslant 50$ and $10^3 \leqslant Ra \leqslant 10^5$. Table 2 presents the maximum values of stream function (ψ_{Max}) at Ra = 10^5. It can be observed from Table 2 that the maximum values of stream function (ψ_{Max}) decrease as the Hartmann number increases for all values of Prandtl number. This is because the increase in the magnetic field effect (i.e., Hartmann number increases) causes to reduce the effect of natural convection and as a result the intensity of circulation and the maximum values of stream function decrease.

Table 1 Comparison of average Nusselt number at the hot left sidewall for different grid size and Ha = 0.

Grid size	Ra = 10^3	Ra = 10^4
20 × 20	0.91459	2.228671
40 × 40	0.90741	2.136948
60 × 60	0.90105	2.143083
80 × 80	0.90383	2.199452
100 × 100	0.90384	2.199453

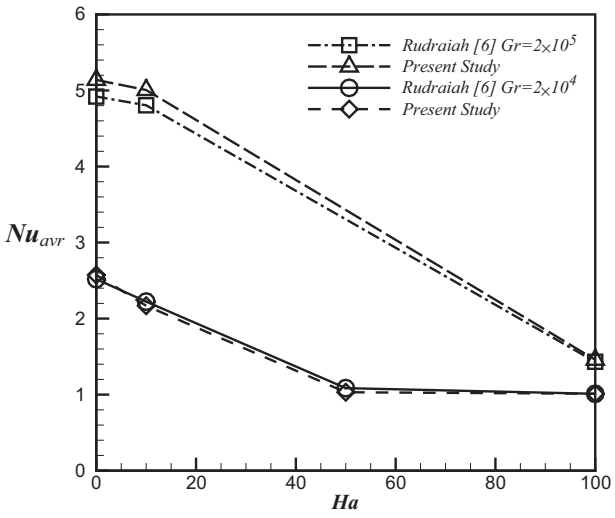

Figure 2 Average Nusselt number versus Hartmann number at different Grashof number.

Table 2 The maximum values of stream function (ψ_{Max}) at Ra = 10^5.

Ha	Pr		
	0.05	0.5	5
0	13.1789	12.849	11.4697
10	13.1057	12.2896	7.04842
50	11.7718	3.06831	1.64664

3.1. Effect of Prandtl number

The streamlines and isotherms for various Prandtl and Hartmann numbers at Ra = 10^3 are displayed in Figs. 3–8. When the Prandtl number is low (i.e., Pr = 0.05 and 0.5), the flow and thermal fields are governed by the effects of both Hartmann number and Rayleigh numbers. The effects of these parameters will be discussed later in detail. The flow field can be represented by primary rotating symmetrical vortices around the adiabatic square body. When the Rayleigh number is low (i.e., Ra = 10^3) and in the absence of magnetic field effect (i.e., Ha = 0), the flow field is governed by the buoyancy force only due to natural convection and this is the main reason for appearing the primary rotating symmetrical vortices which can be observed around the adiabatic square body. No clear effect can be observed for the Prandtl number on the flow field even when it increases to Pr = 5. The same observation can be noticed when the effect of magnetic field is weak (i.e., Ha = 10). On the other hand, when the effect of magnetic field increases (i.e., Ha = 50) the vortices begin to enlarge in the vertical direction and minor vortices can be noticed upward and downward the adiabatic square body. This result indicates that when the Hartmann number is high,

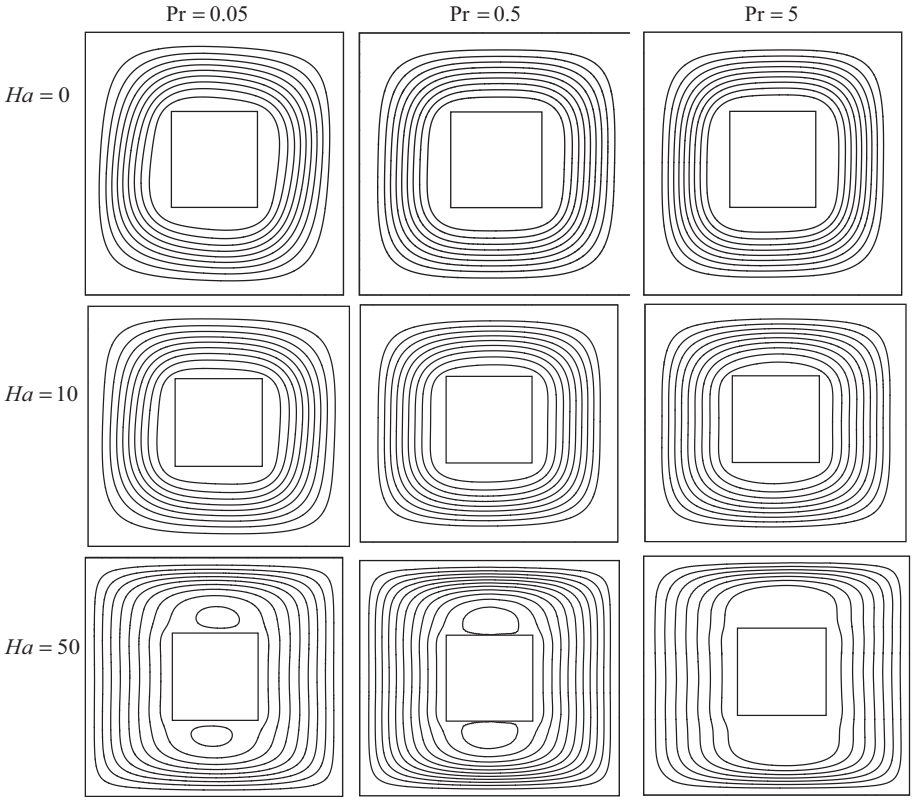

Figure 3 Streamlines for various Hartmann number and Prandtl number for Ra = 10^3.

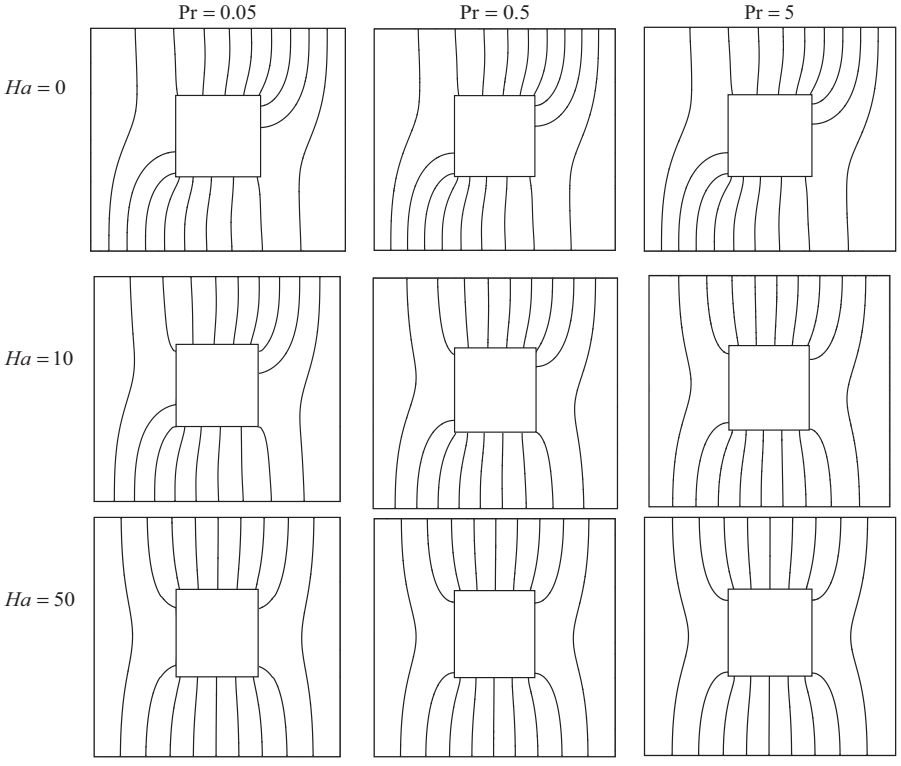

Figure 4 Isotherms for various Hartmann number and Prandtl number for Ra = 10^3.

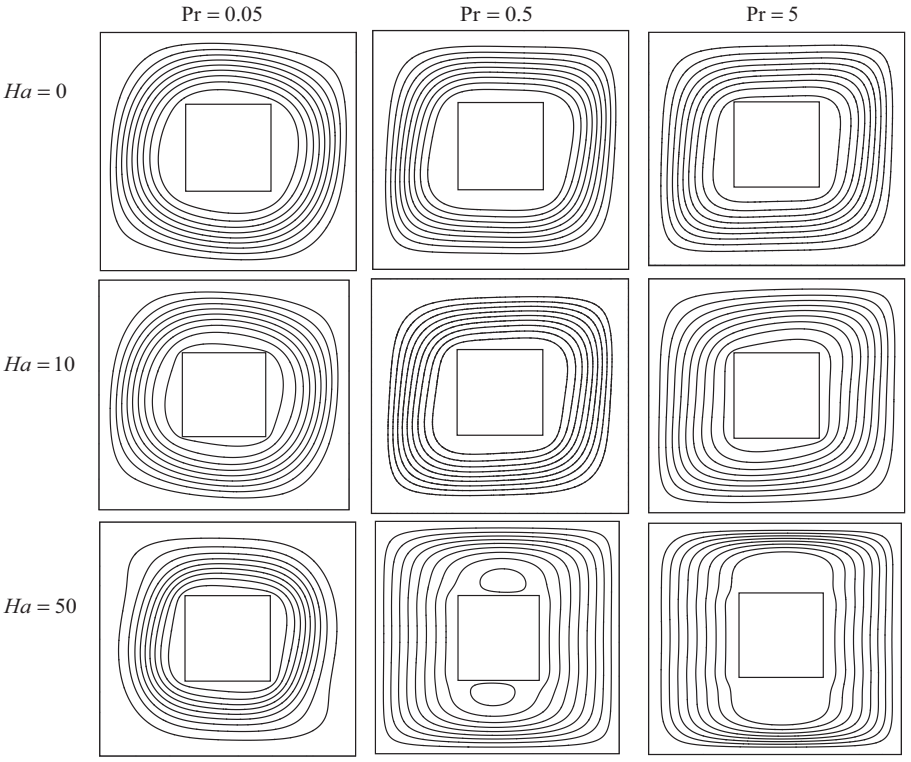

Figure 5 Streamlines for various Hartmann number and Prandtl number for Ra = 10^4.

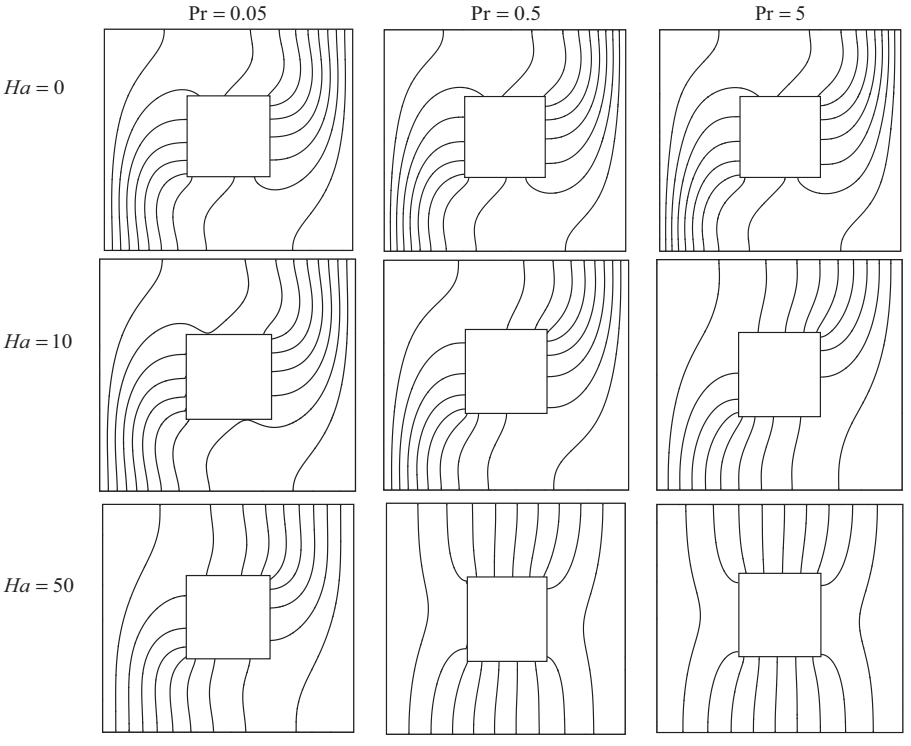

Figure 6 Isotherms for various Hartmann number and Prandtl number for Ra = 10^4.

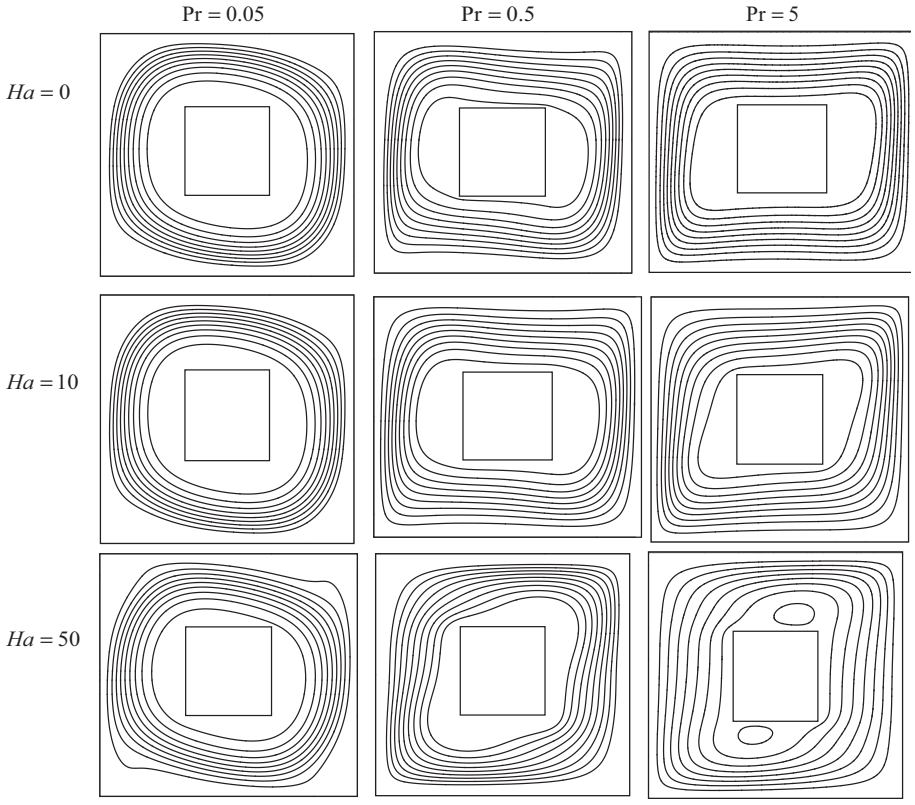

Figure 7 Streamlines for various Hartmann number and Prandtl number for Ra = 10^5.

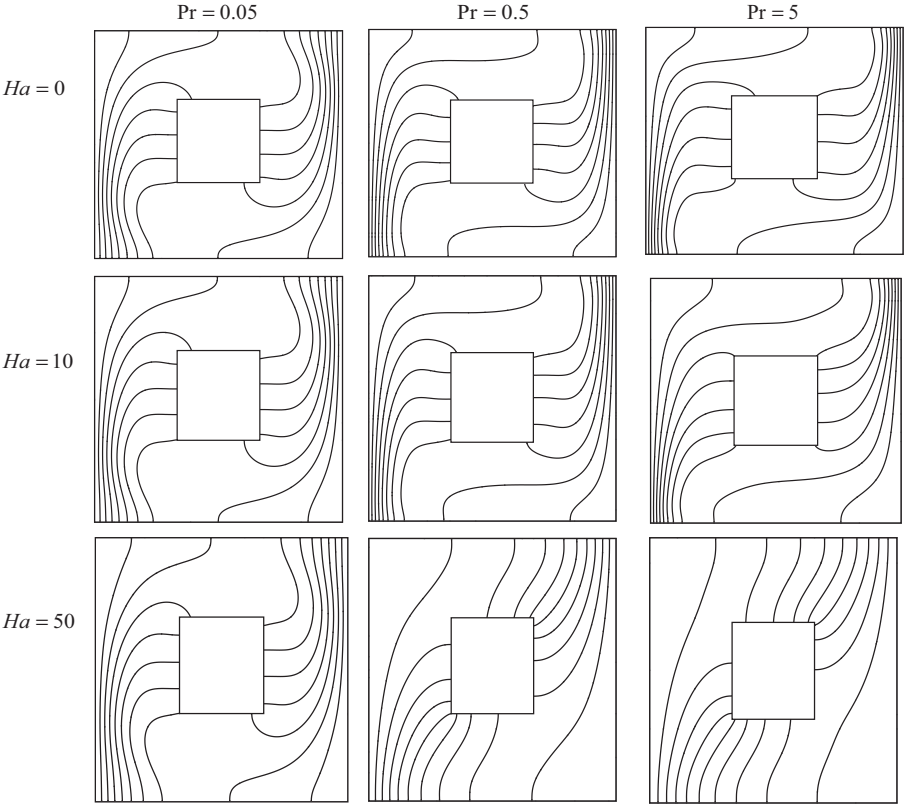

Figure 8 Isotherms for various Hartmann number and Prandtl number for Ra = 10^5.

the magnetic field has a significant effect on the flow field especially when the Prandtl number increases. The same observation can be noticed in Table 1. Furthermore, similar results can be found in Fig. 5 when Ra = 10^4 except that the axis of rotating vortices begins to shift slightly and this movement becomes more clear as the Prandtl number increases. As the Rayleigh number increases to Ra = 10^5 as shown in Fig. 7, the intensity of flow circulation increases and more disturbance occurs in the rotating vortices shape due to strong effect of convection when the Rayleigh number increases while the distance between the rotating vortices and the adiabatic square body begins to decrease as the Prandtl number increases. The flow circulations are stronger near the enclosure center and weak at the hot left and cold right sidewalls due to no slip boundary conditions. In addition, minor vortices can be observed upward and downward the adiabatic square body when both Hartmann number and Prandtl number increase. With respect to isotherms, they are in general similar for all the considered range of Prandtl number when both effects of magnetic field and buoyancy force are slight. As the buoyancy force effect increases by increasing the Rayleigh number a significant confusion can be noticed in the isotherms shape especially when the effect of magnetic field is negligible and the Prandtl number increases. This is because the high flow circulation causes the isotherms to be concentrated near the hot left sidewall and the heat transfer occurs by convection.

3.2. Effect of Hartmann number

The effect of Hartmann number on streamlines and isotherms for various Hartmann numbers (Ha = 0, 10 and 50) and Prandtl number (Pr = 0.05, 0.5 and 5) at Ra = 10^3, 10^4 and 10^5 is illustrated in Figs. 3–8. The Hartmann number represents a measure of the relative importance of MHD flow. As mentioned above, the flow field can be represented by major rotating symmetrical vortices around the adiabatic square body of higher strength near the hot left and cold right sidewalls of the enclosure. The flow field around the interior adiabatic square enclosure is created near the hot left sidewall of the outer enclosure due to temperature difference between the hot left and cold right sidewalls and then hits with the upper adiabatic wall leading to change its direction toward the right cold sidewall and then hits with the adiabatic lower wall. This recycles movement causes to produce the major vortices around the interior adiabatic square enclosure. When the magnetic field effect is negligible (Ha = 0) or weak (i.e., Ha = 10), the intensity of circulation is high, because the buoyancy force due to natural convection is the only dominant force inside the enclosure. From the other side, when the magnetic field effect is significant (i.e., Ha = 50), the Lorentz force due to magnetic field effect becomes higher than the buoyancy force due to natural convection effect which leads to decrease the flow circulation strength and as a result the convection effect diminishes. With respect to isotherms, when the magnetic field effect is negligible (Ha = 0) and the Rayleigh number is low (i.e., Ra = 10^3), the isotherms are in general symmetrical for all values of Prandtl number. The same effect can be noticed when the Hartmann number increases except that the isotherm lines begin to converge from each other. This convergence in the isotherms increases as the Hartmann number increases. When the Rayleigh number increases (i.e., Ra = 10^4 and Ra = 10^5), a clear disturbance can be observed in the isotherms especially when the Hartmann number is zero and the Prandtl number increases. However, as the Hartmann number increases the disturbance in the isotherms begins to decrease gradually. The isotherm lines in this case are in general similar and parallel to the cold right and hot left sidewalls which indicate a strong effect of conduction heat transfer.

3.3. Effect of Rayleigh number

The streamlines and isotherms at different Rayleigh numbers ranging from 10^3 to 10^5 and $0.05 \leqslant Pr \leqslant 5$, $0 \leqslant Ha \leqslant 50$ are shown in Figs. 3–8 when the enclosure left and right sidewalls are maintained at hot and cold temperatures respectively while the bottom and the top walls are kept thermally insulated together with the interior adiabatic square body. When the value of Rayleigh number is low (i.e., Ra = 10^3), the intensity of circulation is very low and the flow vortices around the interior adiabatic square body are in general symmetrical due to weak effect of natural convection and buoyancy force. But, as values of the Rayleigh number increase (i.e., Ra = 10^4 and 10^5), the fluid circulation inside the enclosure is strongly increased and the effect of the convection becomes more dominant. This indicates that the flow circulation becomes stronger as natural convection is dominated and becomes weaker as natural convection effect is decreased. Furthermore, when Ra = 10^5 a clear confusion occurs in the shape of rotating vortices especially when the Hartmann number and Prandtl number increase and minor vortices can be observed upward and downward the interior adiabatic square body. For isotherms, when the Rayleigh number is low (i.e., Ra = 10^3), they are in general smooth and approximately parallel to the cold right and hot left sidewalls and the heat is transferred by conduction. When the Rayleigh number increases (i.e., Ra = 10^4 and 10^5) the isotherms become nonlinear and the heat is transferred due to convection.

3.4. Average Nusselt number

The average Nusselt number for various values of Hartmann number, Prandtl number and Ra = 10^3, Ra = 10^4 and

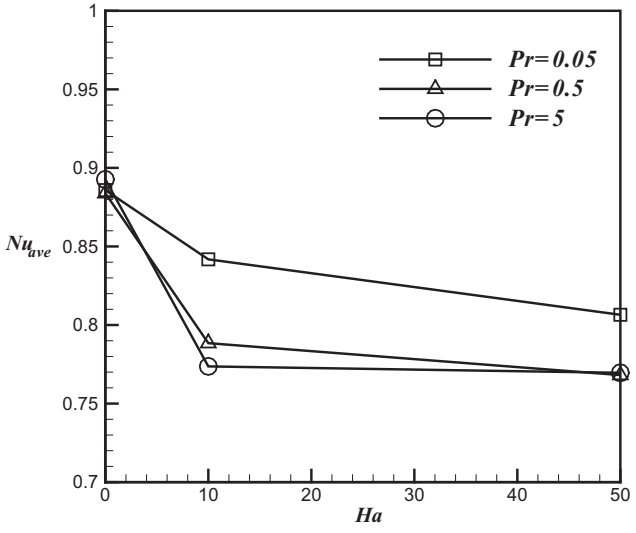

Figure 9 Average Nusselt number for various values of Hartmann number and Prandtl number and Ra = 10^3.

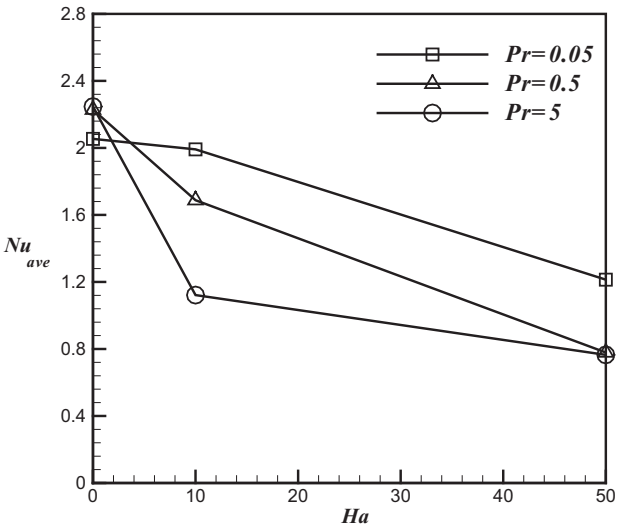

Figure 10 Average Nusselt number for various values of Hartmann number and Prandtl number and Ra = 10^4.

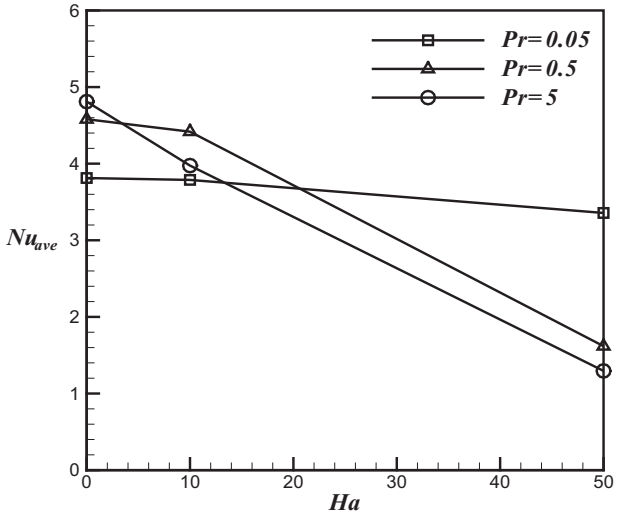

Figure 11 Average Nusselt number for various values of Hartmann number and Prandtl number and Ra = 10^5.

Ra = 10^5 is shown respectively in Figs. 9–11. It is found that the average Nusselt number decreases when the Hartmann number increases. Also, the maximum value of the average Nusselt number occurs when the Prandtl number is high and Hartmann number is zero (i.e., the magnetic field is absence). Therefore, the high average Nusselt number corresponds to the low Hartmann number and vise versa. This is due to the reduction in the temperature gradient when the Hartmann number increases. This reduction leads to decrease the average Nusselt number values. Also, it can be seen from this figure that the average Nusselt number decreases when the Hartmann number increases for all values of Prandtl number. This is because the effect of magnetic field becomes very significant with increasing Hartmann number to reduce the flow circulation strength and reduces the temperature gradient and for this reason the average Nusselt number decreases. From the other hand, it can be seen that the average Nusselt number increases when the Rayleigh number increases. The reason of this behavior is due to increasing the intensity of circulation and the convection effect when the Rayleigh number increases. Therefore, the temperature gradient increases and leads to increase the average Nusselt number.

4. Conclusions

The magneto-hydrodynamic natural convection phenomenon with Prandtl number effect inside a square enclosure having an adiabatic square body was numerically investigated. The effects of various Hartmann number, Rayleigh number and Prandtl number on the flow and thermal fields were analyzed and interpreted. The following conclusions can be detected from the present work results.

1. For the lowest value of Prandtl number and when the magnetic field effect is negligible, the flow and thermal fields are governed by the buoyancy force only. Therefore, the flow field can be represented by primary rotating symmetrical vortices around the adiabatic square body.
2. For all values of Prandtl number, the maximum values of stream function (ψ_{Max}) decrease as the Hartmann number increases
3. The flow vortices begin to enlarge in the vertical direction and minor vortices were observed upward and downward the adiabatic square body when the Hartmann number increases.
4. When the Hartmann number is high; the magnetic field has a strong influence on the flow field especially when the Prandtl number is high.
5. For Hartmann numbers up to 10, the flow field is slightly affected by MHD effects. In this range, in which inertial forces dominate with respect to magnetic forces. From the opposite side, when the Hartmann numbers jump to 50, MHD forces dominate while inertial forces become insignificant.
6. The intensity of circulation increases when the Rayleigh number increases at all values of Hartmann number and Prandtl number. From the other hand, it decreases when the Hartmann number increases at all values of Rayleigh number and Prandtl number.
7. The maximum value of the average Nusselt number is found when the Prandtl number is high and Hartmann number is zero. Also, the average Nusselt number increases when the Rayleigh number increases.

References

[1] D. Fidaros, A. Grecos, N. Vlachos, Development of numerical tool for 3D MHD natural convection, ANNEX XX, pp: 73–74.
[2] M. Sathiyamoorthy, A. Chamkha, Effect of magnetic field on natural convection flow in a liquid gallium filled square cavity for linearly heated side wall(s), Int. J. Therm. Sci. 49 (2010) 1856–1865.
[3] S. Alchaar, P. Vasseur, E. Bilgen, Natural convection heat transfer in a rectangular enclosure with a transverse magnetic field, J. Heat Transfer 117 (1995) 668–673.
[4] J. Garandet, T. Alboussiere, R. Moreau, Buoyancy drive convection in a rectangular enclosure with a transverse magnetic field, Int. J. Heat Mass Transf. 35 (1992) 741–748.

[5] H. Ozoe, K. Okada, The effect of the direction of the external magnetic field on the three-dimensional natural convection in a cubic enclosure, Int. J. Heat Mass Transf. 32 (1989) 1939–1953.
[6] N. Rudraiah, R. Barron, M. Venkatachalappa, C. Subbaraya, Effect of a magnetic field on free convection in a rectangular enclosure, Int. J. Eng. Sci. 33 (1995) 1075–1084.
[7] M. Cowley, Natural convection in rectangular enclosures of arbitrary orientation with magnetic field vertical, Magnetohydrodynamics 32 (1996) 390–398.
[8] N. Al-Najem, K. Khanafer, M. El-Refaee, Numerical study of laminar natural convection in tilted enclosure with transverse magnetic field, Int. J. Numer. Methods Heat Fluid Flow 8 (1998) 651–672.
[9] M. Teamah, Hydro-magnetic double-diffusive natural convection in a rectangular enclosure with imposing an inner heat source or sink, Alex. Eng. J. 45 (4) (2006) 401–415.
[10] M. Ece, E. Buyuk, Natural convection flow under a magnetic field in an inclined rectangular enclosure heated and cooled on adjacent walls, Fluid Dyn. Res. 38 (5) (2006) 546–590.
[11] J. Jalil, K. Al-Tae'y, MHD turbulent natural convection in a liquid metal filed square enclosure, Emirates J. Eng. Res. 12 (2) (2007) 31–40.
[12] S. Saravanan, P. Kandaswamy, Low Prandtl number magnetoconvection in cavities: Effect of variable thermal conductivity, Zeitschrift für angewandte Mathematik und Mechanik 80 (8) (2000) 570–576.
[13] A. Gelfgat, P. Bar-Yoseph, The effect of an external magnetic field on oscillatory instability of convective flows in a rectangular cavity, Phys. Fluids 13 (8) (2001) 2269–2278.
[14] S. Aleksandrova, S. Molokov, Three-dimensional buoyant convection in a rectangular cavity with differentially heated walls in a strong magnetic field, Fluid Dyn. Res. 35 (2004) 37–66.
[15] B. Hof, A. Juel, T. Mullin, Magnetohydrodynamic damping of oscillations in low-Prandtl-number convection, J. Fluid Mech. 545 (2005) 193–201.
[16] J. Lee, M. Ha, A numerical study of natural convection in a horizontal enclosure with a conducting body, Int. J. Heat Mass Transf. 48 (2005) 3308–3318.
[17] J. Jalil, T. Murtadha, K. Al-Tae'y, Z. Huang, Three-dimensional computation of turbulent natural convection in the presence of magnetic field, J. Indian Inst. Sci. 86 (2006) 705–721.
[18] M. Ece, E. Büyük, Natural convection flow under a magnetic field in an inclined square enclosure differentially heated on adjacent walls, Meccanica 42 (5) (2007) 435–449.
[19] D. Henry, A. Juel, H. Ben Hadid, S. Kaddeche, Directional effect of a magnetic field on oscillatory low Prandtl number convection, Phys. Fluids 20 (2008) 1–12.
[20] M. Pirmohammadi, M. Ghassemi, Effect of magnetic field on convection heat transfer inside a tilted square enclosure, Int. Commun. Heat Mass Transfer 36 (2009) 776–780.
[21] H. Ashorynejad, M. Farhadi, K. Sedighi, A. Hasanpour, Natural convection in a porous medium rectangular cavity with an applied vertical magnetic field using Lattice Boltzmann Method, in: 2nd International Conference on Mechanical, Industrial, and Manufacturing Technologies (MIMT 2011), 2011, pp. V1-628–V1-632.
[22] R. Nasrin, Finite element simulation of hydromagnetic convective flow in an obstructed cavity, Int. Commun. Heat Mass Transfer 38 (2011) 625–632.
[23] G. Sheikhzadeh, A. Fattahi, M. Mehrabian, Numerical study of steady magneto-convection around an adiabatic body inside a square enclosure in low Prandtl numbers, Heat Mass Transf. 47 (2011) 27–34.
[24] G. Shit, M. Roy, Hydromagnetic effect on inclined peristaltic flow of a couple stress fluid, Alex. Eng. J. 53 (4) (2014) 949–958.
[25] S. Nadeem, R. Ul Haq, N. Sher Akbar, Z. Khan, MHD three-dimensional Casson fluid flow past a porous linearly stretching sheet, Alex. Eng. J. 52 (4) (2013) 577–582.
[26] M. Qasim, Heat and mass transfer in a Jeffrey fluid over a stretching sheet with heat source/sink, Alex. Eng. J. 52 (4) (2013) 571–575.
[27] M. Teamah, Numerical simulation of double diffusive natural convection in rectangular enclosure in the presences of magnetic field and heat source, Int. J. Therm. Sci. 47 (3) (2008) 237–248.
[28] M. Teamah, A. Elsafty, M. Elfeky, E. El-Gazzar, Numerical simulation of double-diffusive natural convective flow in an inclined rectangular enclosure in the presences of magnetic field and heat source Part A: effect of Rayleigh number and inclination angle, Alex. Eng. J. 50 (2011) 269–282.
[29] M. Teamah, A. Elsafty, E. Massoud, Numerical simulation of double-diffusive natural convective flow in an inclined rectangular enclosure in the presence of magnetic field and heat source, Int. J. Therm. Sci. 52 (2012) 161–175.
[30] M. Teamah, W. El-Maghlany, Augmentation of natural convective heat transfer in square cavity by utilizing nanofluids in the presence of magnetic field and uniform heat generation/absorption, Int. J. Therm. Sci. 58 (2012) 130–142.
[31] M. Teamah, M. Sorour, W. El-Maghlany, A. Afifi, Numerical simulation of double diffusive laminar mixed convection in shallow inclined cavities with moving lid, Alex. Eng. J. 52 (3) (2013) 227–239.
[32] A. Mezrhab, M. Bouzidi, P. Lallemand, Hybrid lattice Boltzmann finite-difference simulation of convective flows, Comput. Fluids 33 (2004) 623–641.
[33] A. Mezrhab, M. Jami, M. Bouzidi, P. Lallemand, Analysis of radiation–natural convection in a divided enclosure using the lattice Boltzmann method, Comput. Fluids 36 (2007) 423–434.
[34] D. Martinez, S. Chen, W. Matthaeus, Lattice Boltzmann magneto hydrodynamics, Phys. Plasmas 6 (1994) 1850–1867.
[35] K. Cramer, S. Pai, Magnatofluid Dynamics for Engineers and Physicists, McGraw-Hill Book Company, New York, 1973.
[36] P. Dellar, Lattice kinetic schemes for magnetohydrodynamics, J. Comput. Phys. 179 (2002) 95–126.